Modeling the Growth of Sugar Kelp (*Saccharina latissima*) in Aquaculture Systems using Dynamic Energy Budget Theory

Celeste T. Venolia[a], Romain Lavaud[b], Lindsay A. Green-Gavrielidis[c,d], Carol Thornber[c], and Austin T. Humphries[a,e*]

[a] Department of Fisheries, Animal and Veterinary Sciences, University of Rhode Island, Kingston, Rhode Island

[b] Institut des Sciences de la Mer, Université du Québec à Rimouski, Rimouski, QC, Canada

[c] Department of Natural Resources Science, University of Rhode Island, Kingston, Rhode Island

[d] *Present address:* Department of Biology and Biomedical Sciences, Salve Regina University, Newport, RI, USA

[e] Graduate School of Oceanography, University of Rhode Island, Narragansett, Rhode Island

* Corresponding Author.

Email Address: humphries@uri.edu (Austin Humphries)

24 **Keywords**

25 Macroalgae; food production; bioenergetics; synthesizing units; Rhode Island

Abstract

Aquaculture is an industry with the capacity for further growth that can contribute to sustainable food systems to feed an increasing global population. Sugar kelp (*Saccharina latissima*) is of particular interest for farmers as a fast-growing species that benefits ecosystems as a primary producer. However, as a new industry in the U.S., farmers interested in growing *S. latissima* lack data on growth dynamics. To address this gap, we calibrated a Dynamic Energy Budget (DEB) model to data from the literature and field-based growth experiments in Rhode Island (U.S.A.). Environmental variables forcing model dynamics include temperature, irradiance, dissolved inorganic carbon concentration, and nitrate and nitrite concentration. The modeled estimates for field *S. latissima* blade length were accurate despite underestimation of early season growth. In some simulations, winter growth was limited by the rate at which the light-dependent reaction of photosynthesis, the first step of carbon assimilation, was performed. Nitrogen (N) reserves were also an important limiting factor especially later in the spring season as irradiance increased, although the low resolution of N forcing concentrations might restrict the model accuracy. Since this model is focused on *S. latissima* grown in an aquaculture setting with winter and spring growth, no specific assumptions were made to include summer growth patterns such as tissue loss or reproduction. The results indicate that this mechanistic model for *S. latissima* captures growth dynamics and blade length at the time of harvest, thus it could be used for spatial predictions of *S. latissima* aquaculture production across a range of environmental conditions and locations. The model could be a particularly useful tool for further development of sustainable ocean food production systems involving seaweed.

1. Introduction

Aquaculture is currently the fastest growing food production sector in the world and is likely to become the main seafood supply in the future (FAO, 2018). In open systems of fed species, aquaculture activities can cause concentrated fluxes of feces and feed wastage leading to eutrophication (Wu, 1995) and alteration of food webs (Herbeck et al., 2013). Open aquaculture systems composed of species that do not require supplemental feed or nutrients (i.e., primary producers and filter feeders) avoid these harms and instead can provide important ecosystem services such as removing dissolved organic and inorganic nutrients (Alleway et al., 2019). Seaweeds are of particular interest as they mitigate hypoxia from terrestrial food production systems and even protect shorelines through dampening of wave energy (Duarte et al., 2017). Outside of these ecosystem services, growing seaweed has been proposed as a way to engage a wider public audience with climate change via offsetting carbon emissions (Froehlich et al., 2019). Seaweed aquaculture has the potential to generate net positive environmental and social impacts, but this industry has been traditionally concentrated in Asian countries (FAO, 2018).

The U.S. does not produce enough aquatic plants to even register in the global production statistics (< 0.1%; FAO, 2018). In the Northeast U.S., sugar kelp (*Saccharina latissima*) is a local species of recent interest for food, biofuel, bioremediation, and pharmaceutical products (Forbord et al., 2012). In a single season of aquaculture growth, *S. latissima* blades can grow up to 60-140 cm depending on the water depth, planting time, and nutrient availability (Handå et al., 2013). Oysters, however, are the most widely aquacultured species in coastal areas of the U.S (NMFS, 2018). The Eastern oyster (*Crassostrea virginica*) mostly grows during the summer months when water temperatures are above 15 °C and is in a state of relative dormancy in the winter (Dame, 1972). It has been suggested that cultivation of *S. latissima* could complement

71 oyster farming because of the differences in growing season with kelp growing mainly when
72 water temperatures are below 15 °C. Therefore, kelp could provide an additional source of
73 income without interfering with oyster production. This new industry, however, would benefit
74 from production estimates in order to assess the biological and economic sustainability of *S.*
75 *latissima* farming.
76 Bioenergetic models can provide such production estimates by studying energy fluxes
77 and usage between the environment and the organism and within the organism. They constitute
78 useful tools in the early development of an aquaculture activity to: assess the carrying capacity of
79 a system before installing new farms (Grant et al., 2007; Filgueira et al., 2014), estimate
80 production and feeding ration (Cho and Bureau, 1998), or to optimize integrated multi-trophic
81 aquaculture (IMTA) systems (Ren et al., 2012). Forcing variables in bioenergetic modelling
82 frameworks are of prime importance as they define the system response. In the case of *S.*
83 *latissima*, blade growth is mainly influenced by irradiance, temperature, and nutrient
84 concentration (Boden, 1979). Other factors such as wave action (Buck and Buchholz, 2005) and
85 ambient light regime (Gerard, 1988) may also determine growth dynamics. In a simple predictive
86 model, Petrell et al. (1993) estimated growth of *S. latissima* using a linear relationship with
87 dissolved inorganic nitrogen concentration and a temperature correction. This model required an
88 assumption that nitrogen dynamics are always limiting growth, thus ignoring the potential
89 influence of irradiance. While integrating photosynthetic processes into a model can be
90 challenging, mechanistic approaches may be more suited to capture the physiological response to
91 environmental variability, especially in a changing environment (Denny and Helmuth, 2009).
92 Dynamic energy budget (DEB) theory provides a sound mechanistic basis for
93 understanding an organism's energetics, which is used to model the flow of mass and energy

94 through an organism from uptake to usage for maintenance, growth, reproduction, or excretion
95 (Kooijman, 2010). This theory of metabolic organization provides a framework to examine the
96 interactive effects of environmental nutrient concentrations and irradiance on an organism
97 through parallel systems of nitrogen (N) and carbon (C) dynamics. Modeling autotrophs is a less
98 common direction for the application of DEB theory. Thus, multiple reserves are necessary to
99 accurately model matter and energy dynamics because of the different nutrient uptake pathways
100 (Kooijman, 2010). Autotroph DEB models have been constructed for microalgae (Lorena et al.,
101 2010, Livanou et al., 2019), phytoplankton-zooplankton interactions (Poggiale et al., 2010),
102 calcification of a coccolithophore (Muller and Nisbet, 2014), and recently the macroalga *Ulva*
103 *lactuca* (Lavaud et al., 2020). Broch and Slagstad (2012) were the first to develop a dynamic
104 bioenergetic model for *S. latissima*, borrowing concepts from DEB theory with the aim of
105 creating a tool for optimizing aquaculture production of Norwegian *S. latissima*. These authors
106 based their model structure on a Droop's cell quota model completed by numerous empirical and
107 allometric relationships to simulate growth of *S. latissima,* but this simplification did not increase
108 parsimony (i.e., reduce the number of model parameters). Using a DEB framework, however,
109 ensures theoretical coherence (i.e., mechanistic description of metabolic processes) and ease of
110 model transference to other regions through less re-calibration.
111 Our objective with this study is to develop a bioenergetic model for *S. latissima* growth
112 using the mechanistic properties of DEB theory. Specifically, we aim to calibrate the macroalga
113 DEB model presented by Lavaud et al. (2020) to field data on kelp from Rhode Island (U.S.A.).
114 The application of this model to another species from a different environment constitutes an
115 important step in the validation of this model structure. The resulting model allows for growth

predictions based on environmental inputs and has the potential to support the sustainable aquaculture industry, particularly with regard to site selection.

2. Methods

2.1 Dynamic Energy Budget model assumptions

The *S. latissima* model is based on a DEB model developed for sea lettuce by Lavaud et al. (2020). The core structure of the *S. latissima* model tracks the uptake of carbon (C) and nitrogen (N), their assimilation into specific reserves and allocation to growth or maintenance or their excretion (Figure 1). The variables that depict the state of the model are the mass of structure M_V (in mol V, moles of structure), Nitrogen reserve density m_{E_N} (in mol N per mol V), and Carbon reserve density m_{E_C} (in mol C per mol V). The code for this model is freely available at https://github.com/CVenolia/SugarKelpDEB.

A core assumption of DEB theory, strong homeostasis, maintains that reserve and structure have constant chemical compositions (Kooijman, 2010). This does not mean that there are always constant amounts of reserve and structure; rather, the amount of carbon, nitrogen, hydrogen, and oxygen relative to each other within specific reserves or structures remains constant.

Two substrates and associated reserves were considered in this *S. latissima* model: C and N (nitrate and nitrite, collectively); other potential nutrients such as phosphorous or potassium were dismissed based on the fact that in regions where nitrogen is not abundant year-round, nitrogen availability is what drives accelerated growth in winter and early spring (Gagné et al., 1982). Adding further reserves to the model would increase complexity by increasing the number

of state variables and parameters with potentially little to no increase in accuracy. On the C side of the model, since *S. latissima* and other algae use carbonic anhydrase to assimilate bicarbonate and convert it into carbon dioxide (Axelsson et al., 2000), we assumed that assimilating carbon dioxide directly was identical to assimilating carbon dioxide that was formed extracellularly from bicarbonate through a carbon concentrating mechanism.

Another assumption of this DEB model is that *S. latissima* is a V1-morph. In DEB theory, V1-morphs are organisms whose surface area is proportional to volume (Kooijman, 2010). *S. latissima* grows as a sheet in both length and width directions at the meristematic blade region near the stipe (Sjøtun, 1993). Variation in blade thickness over an individual blade and through time does not have a substantial impact on the surface area to volume ratio (Vettori and Nikora, 2017) to preclude the V1-morph assumption. Drag from water speed has been found to impact blade morphology (Buck and Buchholz, 2005) but this difference in appearance should not affect the surface area to volume ratio either.

Other assumptions were grounded in the fact that this model was used to determine aquaculture production, which is currently limited in time to November-May. Energy was not used for reproduction or maturity in this model, a simplification that allows for a more parsimonious model. There is evidence suggesting that kelp produces inhibitors that minimize the formation of reproductive tissue during the rapid growth phase (Buchholz and Lüning, 1999, Lüning et al., 2000). Moreover, only a small subset of blades show reproductive development by the time the aquaculture harvest occurs in spring, towards the end of the first period of rapid growth. Furthermore, the aquaculture season of *S. latissima* is set up to maximize growth while minimizing loss or degradation of tissues due to various stresses. Apical frond loss in kelp is correlated with temperature stress and wave action (Krumhansl et al., 2014), mechanical stress of

biofouling (Brown et al., 1997), and overall blade length (Sjøtun, 1993). A tissue loss function would be necessary to accurately model *S. latissima* growth year-round, however, the exact mechanism for this loss remains context-specific in the literature. Aquaculture farmers generally harvest kelp before biofouling begins, which maximizes harvestable blade length and product quality. Photoinhibition may occur in *S. latissima* when high light conditions are combined with high temperature conditions (Heinrich et al., 2012), but since we limit the application of our model to winter-spring seasons, photoinhibition was not accounted for. Photorespiration was not included either to simplify model dynamics (Kooijman, 2010).

2.2 Model structure

All the equations for this model are based on and detailed in Lavaud et al. (2020; Table 1). *S. latissima* blade length (L_w) was calculated via total dry weight (W_d) using an allometric relationship proposed by Gevaert et al. (2001; Table 1). The change in the three state variables (reserve density of C and N and mass of structure) over time is described by differential equations that where solved using the deSolve package (Soetaert et al., 2010) in R (R Core Team, 2019).

2.3 Model calibration

The parameters of the *S. latissima* DEB model were manually calibrated to fit simultaneously a combination of literature data and field data collected for this study (Table 2). Root mean square error (RMSE) was used as a measure of spread in the residuals for assessing the quality of model predictions compared to each observation data set.

185 2.3.1. Literature data

186 Information about the locations where literature studies were conducted was also
187 included because there are multiple ecotypes of *S. latissima* (Gerard, 1988), which may influence
188 their physiological response (Table 3). Due to a lack of local information on certain aspects of *S.*
189 *latissima* life history traits, this model was calibrated with data across multiple ecotypes of *S.*
190 *latissima*. The Arrhenius relationship parameters were estimated using a least squared non-linear
191 regression on compiled physiological rates from the literature. Prior to the estimation, each data
192 set was standardized by dividing by the averaged value found at the reference temperature (Table
193 3). The nitrate and nitrite uptake parameters, $j_{E_N Am}$ maximum volume specific nitrogen
194 assimilation and K_N half-saturation concentration for NO_3^- and NO_2^- uptake, were calibrated
195 using nitrate uptake data from Espinoza and Chapman (1983). To match the dimensions used by
196 these authors (μmol N^{-1} g_{DW}^{-1} h^{-1}) the volume-specific modeled N uptake was multiplied by
197 M_V/W_d (structural mass divided by dry weight). Photosynthesis parameters, ρ_{PSU} photosynthetic
198 unit (PSU) density, α_I specific photon arrival cross section, $\dot{b}_I$ binding probability of a photon to
199 a free light synthesizing unit, and $\dot{k}_I$ dissociation rate of photosynthetic products, were calibrated
200 using oxygen production data from Johansson and Snoeijs (2002).

201 Appropriate literature data for calibrating several model parameters were not available.
202 For instance, air-based carbon dioxide uptake data for *S. latissima* (Ní Longphuirt et al., 2013)
203 were examined to estimate dissolved inorganic carbon uptake but ultimately were rejected due to
204 likely dissimilarity to submerged uptake. Carbon uptake parameters, maintenance rates, the yield
205 factor of C reserve and the rejection flux were estimated during model testing so as to result in
206 predicted length within the observed range in length data (Table 2). Other parameters such as the
207 reserve turnover rates are difficult to compare to measurable physiological data, so these

208 parameters were set based on previously assumed values by Lorena et al. (2010) and Lavaud et
209 al. (2020).
210
211 2.3.2. Field data
212 *S. latissima* was grown at four oyster farm sites from fall to spring in both 2017-2018
213 (Year 1) and 2018-2019 (Year 2). *S. latissima* seed was raised in aquaria from harvested local
214 reproductive *S. latissima* tissue collected at Ft. Wetherill, RI, following the methods of Redmond
215 et al. (2014), and seed lines were attached to ropes held in place by moorings at each of the
216 farms. The growing sites were split between Narragansett Bay and Pt. Judith Pond, RI (Figure 2).
217 Longlines of *S. latissima* were placed in duplicates at a depth of 1 m at all the growing sites. *S.*
218 *latissima* growth, measured as length and width (cm), was monitored every 20-85 days using a
219 subset of individuals harvested from the longline. The variability in monitoring timing was
220 largely driven by the availability of farmers to assist with logistics as well as weather conditions.
221 Temperature data were collected every fifteen minutes at each site using HOBO®
222 pendant loggers. Water samples were collected when *S. latissima* growth measurements were
223 taken to determine the concentrations of nitrate and nitrite. In year 1, nitrate and nitrite
224 concentrations were measured using a LACHAT Flow Injection Autoanalyzer (LACHAT, 2008,
225 method detection limit 0.3 µM). In year 2, nitrate and nitrite concentrations were determined
226 using an Astoria Pacific Model 303A Segmented Continuous Flow Autoanalyzer (Astoria-
227 Pacific Inc, Clackamas, OR; Eaton et al., 1998, method detection limit 1.43 µM). Because
228 Narragansett Bay S data were below the method detection limit for the analysis done in year 2,
229 we replaced them with data from the nearby University of Rhode Island Graduate School of

230 Oceanography to better reflect reality; samples were run on an Astoria Analyzer (Reed and
231 Oviatt, 2020, method detection limit of 0.1 µM).
232
233 2.4. Model forcing
234 The *S. latissima* model was forced with temperature, irradiance, dissolved inorganic
235 carbon (DIC) concentration, and nitrate and nitrite concentration data on an hourly time step.
236 Temperature recorded at fifteen-minute intervals at each site was averaged on an hourly basis.
237 Due to difficulties with biofouling on irradiance loggers, we used radiative forcing from the
238 North American Regional Reanalysis (Mesinger et al., 2006) to estimate photosynthetically
239 active radiation (PAR, mol γ m^{-2} h^{-1} or E m^{-2} h^{-1}) using this equation: $\mathrm{PAR} = \mathrm{NSW} * \mathrm{PAR_{frac}} *$
240 $\mathrm{C} * \mathrm{e}^{(-\mathrm{k} * \mathrm{z})} * 3600$, with NSW the net shortwave radiation (W m^{-2}) at the water surface
241 calculated from downward shortwave flux minus upward shortwave flux, PAR_{frac} the fraction of
242 the incident flux useable for photosynthesis (dimensionless), C a conversion factor (µmol γ s^{-1}
243 W^{-1}), k extinction coefficient (m^{-1}), z line depth (m), and 3600 to convert from per second to per
244 hour. We used a value of 4.56 µmol γ s^{-1} W^{-1} for C (Mõttus et al., 2011), a PAR_{frac} of 0.43
245 (Mõttus et al., 2011), a k of 0.46 m^{-1} from past work in Narragansett Bay (Ullman & Codiga,
246 2010), and a z of 1 m as kelp lines were held at a depth of a minimum of 1 m. We used linear
247 interpolation to create an hourly forcing from source data every three hours (Figure 3). All sites
248 had the same base irradiance forcing in one year using this method. DIC concentration data were
249 not collected in this study, so this forcing was estimated from other sources. The Pt. Judith Pond
250 sites were held at a constant DIC value of 1.836 10^{-3} mol DIC L^{-1} based on U.S. Environmental
251 Protection Agency data from Ninigret Pond (J. Grear, unpublished data). The Narragansett Bay
252 sites were held at a constant DIC value of 1.956 10^{-3} mol DIC L^{-1} based on data from Brenton

253 Point (Segarra, 2002). Nitrate and nitrite concentrations were also linearly interpolated on an
254 hourly basis. State variable initial conditions were estimated based on approximate length and
255 weight at planting of the kelp blades (M_V = 0.00164 g_{DW}). Reserve densities had to be assumed
256 but their impact on end results is limited to the first few days of the simulation. Initial $m_{E_C}$was
257 set at 0.002 mol C mol V^{-1} and m_{E_N} at 0.01 mol N mol V^{-1} in year 1 and 0.01 and 0.09,
258 respectively, in year two.
259
260 2.5 Sensitivity Analyses
261 To determine how each DEB parameter influenced simulation outputs, we analyzed the
262 local sensitivity of the three state variables to model parameters using an L1 summary value of
263 sensitivity from the R package FME (Soetaert and Petzoldt, 2010). The larger the L1 metric a
264 parameter has the greater the sensitivity of the state variables to that parameter.
265
266 **3. Results**
267
268 3.1 Model calibration: Literature data
269 The Arrhenius relationship fit to the compiled literature data (Table 3) reflected
270 maximum physiological rates at temperatures around 13 °C (Figure 4). The lower boundary of
271 the temperature tolerance range in the Arrhenius relationship was 0 °C, and the upper boundary
272 was 13.39 °C. The rather low value for the upper boundary indicates that the optimum
273 temperature is close to the upper limit of the tolerance range for this species. However, the shape
274 of the curve past this point implies that the effects of high temperatures on the metabolism of

sugar kelp appear gradually with increasing temperature. The adjusted R-squared for this relationship was 0.55 (p-value = $2.74 * 10^{-11}$).

Using the nitrate uptake data from Espinoza and Chapman's (1983) St. Margaret's Bay site (Nova Scotia, Canada) provided estimates of maximum volume specific nitrate and nitrite assimilation of $1.5 * 10^{-4}$ mol N mol V^{-1} h^{-1} and a half-saturation concentration of $2.5 * 10^{-6}$ mol NO_3^- and NO_2^- L^{-1} (Figure 5). The fit for the data collected at 18 °C was slightly better with a RMSE of 0.374 µmol N g_{DW}^{-1} h^{-1} than the 9 °C data at 0.504 µmol N g_{DW}^{-1} h^{-1}.

For the oxygen production data (Johansson and Snoeijs, 2002) used to calibrate the photosynthesis parameters, the values that had the lowest error around the data were a PSU density ρ_{PSU} = 0.05 mol PSU mol V^{-1}, specific photon arrival cross section α_I of 1 m^2 mol PSU^{-1}, a binding probability of a photon to a free light synthesizing unit $\dot{b}_I$ = 0.5 (dimensionless), and a dissociation rate of photosynthesis products $\dot{k}_I$ = 0.075 mol γ mol PSU^{-1} h^{-1} (Figure 5). The resulting RMSE for this data set was 0.54 mg O_2 g_{DW}^{-1} h^{-1}. The maximum oxygen production rate of the model was approximately 4.95 mg O_2 g_{DW}^{-1} h^{-1} (Figure 5).

3.2 Model calibration: Field data

In year 1, the maximum water temperature recorded at the sites was 16.7 °C in November and the minimum temperature was –1.72 °C in January (Figure 6). For year 2, the maximum temperature was 15.28 °C in May and the minimum temperature was –1 °C in January. Temperature changes were consistent across all four sites for both years.

The nitrate and nitrite concentration forcing variable had a lower resolution than the temperature forcing because of the linear interpolation between the N measurements (Figure 6). The mean N concentration at the Pt. Judith Pond sites was $4.42 * 10^{-6}$ mol NO_3^- and NO_2^- L^{-1} (±

298 2.76 * 10^{-6}) and 2.20 * 10^{-6} mol NO_3^- and NO_2^- L^{-1} (± 2.99 * 10^{-6}) at the Narragansett Bay sites
299 in year 1. For year 2, the mean N concentration at the Pt. Judith Pond sites was 1.01 * 10^{-6} mol
300 NO_3^- and NO_2^- L^{-1} (± 2.11 * 10^{-6}) and 1.87 * 10^{-6} mol NO_3^- and NO_2^- L^{-1} (± 2.97 * 10^{-6}) at the
301 Narragansett Bay sites.
302
303 3.3 Predicted growth and model dynamics
304 *S. latissima* grew quickly with mean elongation across all sites studied of 0.87 ± 0.63 cm
305 d^{-1} in year 1 and 1.18 ± 0.62 cm d^{-1} in year 2 (Figure 7). End of season blade length varied, but
306 no clear trend based on sites was observed (Table 4). The *S. latissima* DEB model generally
307 underestimated growth observed in the early parts of the season (planting to end of March) but
308 accurately predicted the length at harvest within one standard deviation of the observed mean
309 length for the majority of sites (Figure 7). An exception to this trend was the first *S. latissima*
310 line planted at Pt. Judith Pond South in year 1 for which final length was overestimated. The
311 RMSEs for the model length prediction to the field length data ranged widely from 4.01 to 53.94
312 cm (Figure 7). Examining the reject fluxes from the growth SU indicate that the C reserve
313 (carbohydrates) limited model growth after planting for greatly variable time spans across the
314 sites, seasons, and lines (Figure 8). A growth limitation by C reserve may result from low C
315 assimilation due to a low specific relaxation rate. Temperature seemed to be the main factor
316 controlling C assimilation, as indicated by the greater similarity of the shape of the temperature
317 correction to that of C assimilation than the shape of the seasonal trend of irradiance (Figure 9).
318 N limitation seemed to have a strong role in controlling modeled *S. latissima* growth dynamics
319 overall due to the proportion of time C was rejected from the growth SU.

3.4 Sensitivity Analysis

The parameters with the largest effects (>9000 L1 summary value of sensitivity functions) on the state variables were T_0, T_A, T_H, T_L, T_{AH}, T_{AL}, y_{E_CV}, κ_{E_i}, y_{IC}, y_{CO_2C}, and α_I (Figure 10). The parameters $\dot{j}_{E_CAm}$, ρ_{PSU} and $\dot{b}_I$ had a moderate effect with L1 values ranging between 3000-7000. Finally, some parameters showed small but non-zero effects on the state variables, including: y_{E_NV}, $\dot{k_{EC}}$, k_{EN}, j_{CO_2m}, and $\dot{k}_I$ (Figure 10).

4. Discussion

Aquaculture development represents a key role in expanding U.S. sustainable food production and macroalgae can provide high returns when the proper growth conditions exist. Understanding and predicting the growth dynamics of *S. latissima* can provide the aquaculture industry with a powerful predictive tool for estimating production potential. This model is the first attempt to apply Dynamic Energy Budget (DEB) theory to a macroalga of the order Laminariales. The process-based model presented in this study allowed us to better understand growth limitations as they relate to the behavior of the model.

4.1 Growth Limitation

In several model simulations, predictions of early *S. latissima* growth seemed to indicate a limitation in carbon (C) assimilation due to a low modeled specific relaxation rate, j_I, by photosynthetic SU2 processing the light-dependent reactions of photosynthesis. There is some evidence that a lack of C reserve occurs in the field during winter due to lower irradiance; *S. latissima* individuals older than a year were shown to have a decrease in blade C content mid-winter suggesting consumption of stored carbohydrates (Sjøtun, 1993). New sporophytes would

not have this carbohydrate pool to draw upon and would exclusively depend on photosynthesis to acquire C. The decrease in C content observed by Sjøtun (1993) suggests that C dynamics may be limiting *S. latissima* growth, but substrate limitation was not directly examined by this author. In simulations where irradiance was the initial limiting factor for growth, the early season model underestimation of field growth may reflect an outsized impact of the temperature correction of $\dot{k}_I$ on the specific relaxation rate, j_I, in comparison to irradiance. As with many DEB parameters, $\dot{k}_I$ is difficult to estimate directly based on empirical data and our assumption of dependence on temperature as in other algae (Kooijman, 2010; Lavaud et al., 2020) may not be as relevant to *S. latissima*. As ocean temperature seasonal trends trail behind irradiance changes (Brady-Campbell et al., 1984), *S. latissima*'s early season growth could be driven by this early season increase in irradiance rather than water temperature change. More data are necessary to confirm why the *S. latissima* DEB model underestimates winter growth.

Other than an increase in irradiance, day length could also impact seasonal growth patterns. Broch and Slagstad's (2012) *S. latissima* model used the rate of change of day length in a photoperiodic effect function to mimic growth seasonality. These authors relied on the hypothesis that *S. latissima* is a "seasonal anticipator" with endogenous circadian rhythms (Kain, 1989). Seasonal anticipators are posited to grow strategically in response to a trigger. Other kelps such as *Laminaria hyperborea* and *Laminaria digitata* have been shown to have free-running seasonal growth patterns, which suggests control by endogenous circadian rhythms (Schaffelke and Lüning, 1994). Species-specific evidence for this circadian hypothesis is lacking including the mechanism for what would trigger *S. latissima*'s photoperiodic response. If this is the case, substrate uptake or reserve mobilization parameters may be adjusted in the model in response to a trigger to temporarily favor early winter growth.

366 Another possible reason for underestimation of early season C dynamics may be a lack of
367 energy gain at night. *S. latissima*'s carbon dioxide exchange rate is not closely correlated with
368 irradiance because carbon dioxide uptake by the alga continues into the dark (Mortensen, 2017).
369 On average, 11% of *S. latissima*'s carbon fixation happens in the dark (Kremer and Markham,
370 1979). The linkage between the light-dependent and light-independent reactions is modeled in
371 our study as an immediate transference. In other words, when there is no irradiance input, the
372 assimilation of carbohydrates to the C reserve is zero. However, adding this layer of
373 physiological accuracy could reduce model efficiency without increasing predictive capacity.
374 In some instances, N was the limiting factor to growth, as shown by more rejected C by
375 the growth SU, for example, in Pt. Judith Pond sites in Dec and Jan of year 1, resulting in lower
376 predicted length as compared to field observations. The low resolution of N forcing could limit
377 our interpretation of the results, but our N data show general agreement with long-term
378 monitoring at the University of Rhode Island Graduate School of Oceanography (Reed and
379 Oviatt, 2020). The seasonal dynamics of N in Narragansett Bay matches that of many sites
380 around New England with higher concentrations of N in the October-March and reduced summer
381 N concentrations (Townsend 1991, Reed and Oviatt, 2020). Nitrogen has been well-documented
382 as a major force limiting primary production across the ocean (Duce et al., 2008). N limitation of
383 *S. latissima* growth may be a reasonable expectation later in the year as inorganic N availability
384 is thought to facilitate late winter and early spring *S. latissima* growth (Ahn et al., 1998).
385 To increase the ability to accurately understand growth limitation with this DEB model,
386 localized N uptake data in response to changing N concentrations would be useful. Ecotypic
387 differences in N nutrition have been observed both in Nova Scotia (Canada, Espinoza and
388 Chapman, 1983) and when comparing Long Island Sound (New York) kelps with kelps from

389 Maine (Gerard, 1997). In this study, Espinoza and Chapman's (1983) N uptake data from St.
390 Margaret's Bay was chosen for calibration over their Bay of Fundy data because the April-
391 November seasonal depletion of nitrate was more similar to Narragansett Bay conditions than the
392 year-round nitrate replete conditions of the Bay of Fundy. Kelp individuals from St. Margaret's
393 Bay also had greater nitrate accumulation ability (Espinoza and Chapman, 1983). The seasonal
394 dissolved inorganic nitrogen patterns were comparable for the Long Island Sound and Maine
395 kelps that Gerard (1997) analyzed, but the Long Island Sound plants (geographically closer to
396 our kelp from Narragansett Bay) accumulated larger N reserves, which allowed for a ramping up
397 of photosynthetic component production. Such ability to store nitrogen over winter months has
398 been documented (Nielsen et al., 2014) and may explain the observed pattern of C reserve
399 limitation in our model. Year-long simulations would most likely provide different conclusions
400 when N availability in the environment decreases (Reed and Oviatt, 2020).
401 The chemical composition of available N for assimilation may have an effect on N
402 limitation. Nitrate was the primary N source used in this model primarily due to lack of complete
403 ammonium data to include in the forcing. Including ammonium, however, may allow for more
404 accurate predictions of growth dynamics as ammonium has been hypothesized to be a more
405 efficient N source for macroalgae especially in low light conditions because it may be
406 assimilated passively through diffusion (Harrison and Hurd, 2001). One argument for leaving out
407 ammonium is to simplify dynamics, as a different substrate composition would require another
408 reserve pool, although pools of different N forms may be combined and uptake rates for different
409 N sources averaged. Another reason is that *S. latissima* has been shown to have a higher
410 maximum uptake of nitrate compared to ammonium: ammonium saturation was observed at
411 concentrations of 10 μM whereas nitrate saturation was not observed until 30 μM (Ahn et al.,

412 1998). The greater variation in nitrate uptake could cause nitrate to have a more important role in
413 shaping *S. latissima* growth dynamics. The caveat to using these rates to understand dynamics
414 broadly is that kelp individuals used in this study came from ammonium rich and nitrate poor
415 habitat (Ahn et al., 1998), which may have some effect on the reported uptake rates.
416
417 4.2 Sensitivity Analysis
418 The high sensitivity of the state variables to the temperature related parameters is a
419 logical outcome of the central role of temperature in DEB theory. Since the temperature
420 correction is applied to such a large number of rates in the organism, the high sensitivity to these
421 values is reasonable. It is also an argument for caution in regional calibration of the Arrhenius
422 relationship. The sensitivity of the *S. latissima* model to the fraction of rejection flux
423 incorporated back in i-reserve (κ_{E_i}) contrasts with the lack of sensitivity of Lorena et al. (2010)'s
424 microalgae model to the same parameter. Different metabolic pathways, storage capacities, and
425 efficiencies might be responsible for these differences between a phytoplankton species and a
426 macroalgae. More experimental work focusing on the dynamics of internal and external N
427 concentration in controlled settings should help confirm the calibration of this parameter. The
428 sensitivity of the model to the yield factor of C reserve on photons and on CO_2 (y_{IC} and y_{CO_2C}
429 respectively), reflects the generality of photosynthesis reactions; a change in these parameters
430 would involve important modifications of the physiological processes involved in
431 photosynthesis. Since these processes are well known and established, it reinforces our
432 confidence in the model. The high sensitivity of the model to the yield factor of C reserve to
433 structure (y_{E_CV}) in comparison to the small but nonzero impact of the yield factor of N reserve to
434 structure (y_{E_NV}) might be reflective of the greater amount of C reserve required by the chemical

composition of the structure. This greater proportion of C may also be the reason the majority of the impactful parameters are related to C dynamics. The state variables had a small sensitivity to reserve turnover parameters, which calibration may be challenging due to the difficulty to relate these abstract parameters to observed data. It is, therefore, encouraging that the sensitivity to these values was low. This analysis should increase our overall confidence in the values of the calibrated parameters and the reliability of the model as the most sensitive parameters are those in which we can have highest assurance.

4.3 Model Application

Limitations to broader geographic use of this parameter set center around the plasticity of *S. latissima* and the existence of ecotypes in this species. The differentiation of ecotypes occurs when individuals have an acclimation range related to their habitat of origin (Gerard, 1988). For instance, *S. latissima* individuals from New York have been shown to have a different physiological response to temperature in a lab setting than individuals from Maine (Gerard, 1988). In the context of this study, Narragansett Bay (RI, U.S.A.) is located towards the southern boundary of *S. latissima* distribution range (Taylor, 1972); kelps from this location likely have different physiological rates than in northern neighboring states. The existence of multiple ecotypes of this species suggests that some parameters, such as the temperature parameters or maximum assimilation rates of substrates, require regional adjustment, particularly in the Arctic. Additionally, the model assumption regarding the proportionality of surface area to volume impedes prediction of blade shape plasticity, which is a characteristic of *S. latissima* related to drag (Buck and Buchholz, 2005). Since the blade thickness and amount of blade ruffling could impact the relationship between surface area and volume, some adjustments to the model may be

458 warranted in regions where blade plasticity results in thicker thalli as the surface area to volume
459 relationship would be impacted. Determining a mechanism for how blade type changes in
460 response to hydrodynamic conditions would provide a clearer picture of overall growth
461 dynamics.

462 Further research on the mechanisms for frond loss, blade plasticity, and regional
463 parameter information have the potential to improve this DEB model. A better understanding of
464 the physiological cause for apical frond loss would allow this process to be included in
465 mechanistic models in a more meaningful way than modeling erosion as a response to one
466 correlated variable such as length or age. Aging mechanisms within DEB theory (Kooijman,
467 2010), based on the production of harmful compounds may also be of interest to model frond
468 loss. Finally, underwater carbon dioxide uptake data and more regionally appropriate oxygen
469 production data in response to variable irradiance would be useful to better calibrate parameters
470 linked to *S. latissima* photosynthesis.

471 Our model establishes a baseline for *S. latissima* DEB parameters and further testing of
472 the model equations from Lavaud et al. (2020). This tool facilitates analyzing local growth
473 limitations as they relate to modeled responses to changing environmental conditions. Our *S.*
474 *latissima* DEB model is a first step towards estimating kelp aquaculture production in the U.S.A.
475 In future work, this *S. latissima* DEB model could be coupled with a DEB model for *C. virginica*
476 (Lavaud et al., 2017) and the Regional Ocean Modeling System (ROMS) with a Carbon Silicate
477 Nitrogen Ecosystem (CoSiNE) model (Chai et al, 2009) to predict growth potential at sites in the
478 Northeastern U.S.A. Supporting macroalgae aquaculture is an important avenue to work towards
479 the vital goals of feeding a growing human population and while combatting climate change.
480

Acknowledgements

This study would not have been possible without the valuable contributions of the aquaculture farmers working with us to grow kelp for two years: Cindy and John West of Moonstone Oysters, Russ and Thomas Blank of Rome Point Oyster Farm, Trip Whilden of Wickford Oyster Co, and Perry Russo of Matunuck Oyster Farm. Dave Ullman and Chris Kincaid provided assistance in the initial project development. Thomas Guyondet facilitated collaborations around this project. Dawn Outram at the Marine Science Research Facility at URI's Narragansett Bay Campus and Kelly Addy conducted water analyses. Candace Oviatt and Laura Reed shared their nitrogen data, which is funded by EPA, NOAA-CHRP and RI DEM. T. Ben-Horin provided assistance collecting reproductive kelp. J. Barnes, A. Barry, R. Derouin, E. Ferrante, I. Gray, K. Hannibal, C. Jenkins, A. Mauk, L. Sebesta, and A. Wetzel provided lab and field assistance. S. McWilliams, D. Ullman, M. Gomez-Chiarri, L. Josephs, and K. Gorospe provided feedback on previous versions of the manuscript.

Funding: This work is supported by the National Oceanic and Atmospheric Administration Saltonstall-Kennedy grant [17GAR008], NSERC grant [497065-2016], the National Science Foundation under EPSCoR Cooperative Agreement #OIA-165522 and the U.S. Department of Agriculture's National Institute of Food and Agriculture, Hatch Formula project 1011478.

501 **References**

502 Ahn, O., Petrell, R. J., & Harrison, P. J. (1998). Ammonium and nitrate uptake by *Laminaria*
503 *saccharina* and *Nereocystis luetkeana* originating from a salmon sea cage farm. *Journal of*
504 *Applied Phycology*, *10*(4), 333-340.

505 Alleway, H. K., Gillies, C. L., Bishop, M. J., Gentry, R. R., Theuerkauf, S. J., & Jones, R.
506 (2019). The ecosystem services of marine aquaculture: Valuing benefits to people and nature.
507 *BioScience*, *69*(1), 59-68.

508 Axelsson, L., Mercado, J., & Figueroa, F. (2000). Utilization of HCO_3^- at high pH by the brown
509 macroalga *Laminaria saccharina*. *European Journal of Phycology*, *35*(1), 53-59.

510 Boden, G. T. (1979). The effect of depth on summer growth of *Laminaria saccharina*
511 (Phaeophyta, Laminariales). *Phycologia*, *18*(4), 405-408.

512 Bolton, J. J., & Lüning, K. (1982). Optimal growth and maximal survival temperatures of
513 Atlantic *Laminaria* species (Phaeophyta) in culture. *Marine Biology*, *66*(1), 89-94.

514 Brady-Campbell, M. M., Campbell, D. B., & Harlin, M. M. (1984). Productivity of kelp
515 (*Laminaria* spp.) near the southern limit in the northwestern Atlantic Ocean. *Marine Ecology*
516 *Progress Series*, *18*(1), 79-88.

517 Broch, O. J., & Slagstad, D. (2012). Modelling seasonal growth and composition of the kelp
518 *Saccharina latissima*. *Journal of Applied Phycology*, *24*(4), 759-776.

519 Brown, M. T., Nyman, M. A., Keogh, J. A., & Chin, N. K. M. (1997). Seasonal growth of the
520 giant kelp *Macrocystis pyrifera* in New Zealand. *Marine Biology*, *129*(3), 417-424.

521 Buchholz, C., & Lüning, K. (1999). Isolated, distal blade discs of the brown alga *Laminaria*
522 *digitata* form sorus, but not discs, near to the meristematic transition zone. *Journal of Applied*
523 *Phycology*, *11*(6), 579.

524 Buck, B. H., & Buchholz, C. M. (2005). Response of offshore cultivated *Laminaria saccharina*
525 to hydrodynamic forcing in the North Sea. *Aquaculture*, *250*(3-4), 674-691.
526 Chai, F., G. Liu, H. Xue, L. Shi, Y. Chao, C.-M. Tseng, W.-C. Chou, and K.-K. Liu (2009).
527 Seasonal and interannual variability of carbon cycle in South China Sea: A three-dimensional
528 physical-biogeochemical modeling study, *Journal of Oceanography,* 65, 703-720.
529 Cho, C. Y., & Bureau, D. P. (1998). Development of bioenergetic models and the Fish-PrFEQ
530 software to estimate production, feeding ration and waste output in aquaculture. *Aquatic Living*
531 *Resources*, *11*(4), 199-210.
532 Dame, R. F. (1972). The ecological energies of growth, respiration and assimilation in the
533 intertidal American oyster *Crassostrea virginica*. *Marine biology*, *17*(3), 243-250.
534 Davison, I. R. (1987). Adaptation of photosynthesis in *Laminaria saccharina* (Phaeophyta) to
535 changes in growth temperature. *Journal of Phycology*, *23*, 273-283.
536 Davison, I. R., & Davison, J. O. (1987). The effect of growth temperature on enzyme activities in
537 the brown alga *Laminaria saccharina*. *British Phycological Journal*, *22*(1), 77-87.
538 Denny, M., & Helmuth, B. (2009). Confronting the physiological bottleneck: a challenge from
539 ecomechanics. *Integrative and Comparative Biology*, *49*(3), 197-201.
540 Duarte, C. M., Wu, J., Xiao, X., Bruhn, A., & Krause-Jensen, D. (2017). Can seaweed farming
541 play a role in climate change mitigation and adaptation? *Frontiers in Marine Science*, *4*, 100.
542 Duce, R. A., LaRoche, J., Altieri, K., Arrigo, K. R., Baker, A. R., Capone, D. G., ... & Geider, R.
543 J. (2008). Impacts of atmospheric anthropogenic nitrogen on the open ocean. *science*, *320*(5878),
544 893-897.
545 Eaton, A. D., Clesceri L. S., Greenberg A. E., & Franson M. H. (1998) Standard methods for the
546 examination of water and wastewater. APHA, AWWA, and WEF, Washington, DC.

547 Espinoza, J., & Chapman, A. R. O. (1983). Ecotypic differentiation of *Laminaria longicruris* in
548 relation to seawater nitrate concentration. *Marine Biology*, 74(2), 213-218.
549 FAO. 2018. *The State of World Fisheries and Aquaculture 2018 - Meeting the sustainable*
550 *development goals.* Rome. Licence: CC BY-NC-SA 3.0 IGO.
551 Filgueira, R., Guyondet, T., Comeau, L. A., & Grant, J. (2014). A fully-spatial ecosystem-DEB
552 model of oyster (*Crassostrea virginica*) carrying capacity in the Richibucto Estuary, Eastern
553 Canada. *Journal of Marine Systems*, *136*, 42-54.
554 Forbord, S., Skjermo, J., Arff, J., Handå, A., Reitan, K. I., Bjerregaard, R., & Lüning, K. (2012).
555 Development of *Saccharina latissima* (Phaeophyceae) kelp hatcheries with year-round
556 production of zoospores and juvenile sporophytes on culture ropes for kelp aquaculture. *Journal*
557 *of Applied Phycology*, *24*(3), 393-399.
558 Fortes, M. D., & Lüning, K. (1980). Growth rates of North Sea macroalgae in relation to
559 temperature, irradiance and photoperiod. *Helgoländer Meeresuntersuchungen*, *34*(1), 15.
560 Froehlich, H. E., Afflerbach, J. C., Frazier, M., & Halpern, B. S. (2019). Blue Growth Potential
561 to Mitigate Climate Change through Seaweed Offsetting. *Current Biology*, 29, 1-7.
562 Gagné, J. A., Mann, K. H., & Chapman, A. R. O. (1982). Seasonal patterns of growth and
563 storage in *Laminaria longicruris* in relation to differing patterns of availability of nitrogen in the
564 water. *Marine Biology*, *69*(1), 91-101.
565 Gevaert, F., Davoult, D., Creach, A., Kling, R., Janquin, M. A., Seuront, L., & Lemoine, Y.
566 (2001). Carbon and nitrogen content of *Laminaria saccharina* in the eastern English Channel:
567 biometrics and seasonal variations. *Journal of the Marine Biological Association of the United*
568 *Kingdom*, *81*(5), 727-734.

569 Gerard, V. A. (1988). Ecotypic differentiation in light-related traits of the kelp *Laminaria*
570 *saccharina*. *Marine Biology*, *97*(1), 25-36.
571 Gerard, V. A. (1997). The role of nitrogen nutrition in high-temperature tolerance of the kelp,
572 *Laminaria saccharina* (Chromophyta). *Journal of Phycology*, *33*(5), 800-810.
573 Grant, J., Curran, K. J., Guyondet, T. L., Tita, G., Bacher, C., Koutitonsky, V., & Dowd, M.
574 (2007). A box model of carrying capacity for suspended mussel aquaculture in Lagune de la
575 Grande-Entrée, Iles-de-la-Madeleine, Québec. *Ecological modelling*, *200*(1-2), 193-206.
576 Handå, A., Forbord, S., Wang, X., Broch, O. J., Dahle, S. W., Størseth, T. R., ... & Skjermo, J.
577 (2013). Seasonal-and depth-dependent growth of cultivated kelp (*Saccharina latissima*) in close
578 proximity to salmon (*Salmo salar*) aquaculture in Norway. *Aquaculture*, *414*, 191-201.
579 Harrison, P. J., & Hurd, C. L. (2001). Nutrient physiology of seaweeds: application of concepts
580 to aquaculture. *Cahiers de biologie marine*, *42*(1-2), 71-82.
581 Heinrich, S., Valentin, K., Frickenhaus, S., John, U., & Wiencke, C. (2012). Transcriptomic
582 analysis of acclimation to temperature and light stress in *Saccharina latissima* (Phaeophyceae).
583 *PLoS One*, *7*(8), e44342.
584 Herbeck, L.S., Unger, D., Wu, Y., & Jennerjahn, T.C., (2013). Effluent, nutrient and organic
585 matter export from shrimp and fish ponds causing eutrophication in coastal and back-reef waters
586 of NE Hainan, tropical China. *Continental Shelf Research* 57, 92–104.
587 Johansson, G., & Snoeijs, P. (2002). Macroalgal photosynthetic responses to light in relation to
588 thallus morphology and depth zonation. *Marine Ecology Progress Series*, *244*, 63-72.
589 Kain, J. M. (1989). The seasons in the subtidal. *British Phycological Journal*, *24*(3), 203-215.
590 Kooijman, S. A. L. M. (2010). *Dynamic energy budget theory for metabolic organisation*.
591 Cambridge university press.

592 Kremer, B. P., & Markham, J. W. (1979). Carbon assimilation by different developmental stages
593 of *Laminaria saccharina*. *Planta*, *144*(5), 497-501.
594 Krumhansl, K. A., Lauzon-Guay, J. S., & Scheibling, R. E. (2014). Modeling effects of climate
595 change and phase shifts on detrital production of a kelp bed. *Ecology*, *95*(3), 763-774.
596 LACHAT (2008). QuikChem Method 31-107-04-1-A. LACHAT INSTRUMENTS, Loveland,
597 CO.
598 Lavaud, R., La Peyre, M. K., Casas, S. M., Bacher, C., & La Peyre, J. F. (2017). Integrating the
599 effects of salinity on the physiology of the eastern oyster, *Crassostrea virginica*, in the northern
600 Gulf of Mexico through a Dynamic Energy Budget model. *Ecological Modelling*, *363*, 221-233.
601 Lavaud, R., Filgueira, R., Nadeau, A., Steeves, L., & Guyondet, T. (2020). A Dynamic Energy
602 Budget model for the macroalga *Ulva lactuca*. *Ecological modelling*, *418*, 108922.
603 Livanou, E., Lagaria, A., Psarra, S., & Lika, K. (2019). A DEB-based approach of modeling
604 dissolved organic matter release by phytoplankton. *Journal of sea research*, *143*, 140-151.
605 Lorena, A., Marques, G. M., Kooijman, S. A. L. M., & Sousa, T. (2010). Stylized facts in
606 microalgal growth: interpretation in a dynamic energy budget context. *Philosophical*
607 *Transactions of the Royal Society B: Biological Sciences*, *365*(1557), 3509-3521.
608 Lüning, K., Wagner, A., & Buchholz, C. (2000). Evidence for inhibitors of sporangium
609 formation in *Laminaria digitata* (Phaeophyceae) during the season of rapid growth. *Journal of*
610 *Phycology*, *36*(6), 1129-1134.
611 Mesinger, F., G. DiMego, E. Kalnay, K. Mitchell, and Coauthors, 2006: North American
612 Regional Reanalysis. *Bulletin of the American Meteorological Society*, **87**, 343–360.

613 Mortensen, L. M. (2017). Diurnal carbon dioxide exchange rates of *Saccharina latissima* and
614 *Laminaria digitata* as affected by salinity levels in Norwegian fjords. *Journal of Applied*
615 *Phycology*, *29*(6), 3067-3075.
616 Mõttus, Matti & Sulev, Madis & Frederic, Baret & Lopez-Lozano, R. & Reinart, Anu. (2011).
617 Photosynthetically Active Radiation: Measurement and Modeling. In R. Meyers (Ed.),
618 *Encyclopedia of Sustainability Science and Technology* (pp. 7970-8000). New York, NY:
619 Springer.
620 Muller, E. B., & Nisbet, R. M. (2014). Dynamic energy budget modeling reveals the potential of
621 future growth and calcification for the coccolithophore *E miliania huxleyi* in an acidified ocean.
622 *Global change biology*, *20*(6), 2031-2038.
623 National Marine Fisheries Service (2018) Fisheries of the United States, 2017. U.S. Department
624 of Commerce, NOAA Current Fishery Statistics No. 2017 Available at:
625 https://www.fisheries.noaa.gov/feature-story/ fisheries-united-states-2017
626 Ní Longphuirt, S., Eschmann, C., Russell, C., & Stengel, D. B. (2013). Seasonal and species-
627 specific response of five brown macroalgae to high atmospheric CO2. *Marine Ecology Progress*
628 *Series*, 493, 91-102.
629 Nielsen, M.M., Krause-Jensen, D., Olesen, B., Thinggaard, R., Christensen, P.B. and Bruhn, A.,
630 (2014). Growth dynamics of *Saccharina latissima* (Laminariales, Phaeophyceae) in Aarhus Bay,
631 Denmark, and along the species' distribution range. *Marine biology*, *161*(9), 2011-2022.
632 Petrell, R. J., Tabrizi, K. M., Harrison, P. J., & Druehl, L. D. (1993). Mathematical model of
633 *Laminaria* production near a British Columbian salmon sea cage farm. *Journal of Applied*
634 *Phycology*, *5*(1), 1-14.

635 Poggiale, J. C., Baklouti, M., Queguiner, B., & Kooijman, S. A. L. M. (2010). How far details
636 are important in ecosystem modelling: the case of multi-limiting nutrients in phytoplankton–
637 zooplankton interactions. *Philosophical Transactions of the Royal Society of London B:*
638 *Biological Sciences*, *365*(1557), 3495-3507.
639 Raven, J. A., Ball, L. A., Beardall, J., Giordano, M., & Maberly, S. C. (2005). Algae lacking
640 carbon-concentrating mechanisms. *Canadian Journal of Botany*, *83*(7), 879-890.
641 R Core Team (2019). R: A language and environment for statistical computing. R Foundation for
642 Statistical Computing, Vienna, Austria. URL https://www.R-project.org/.
643 Redmond, S., L.A. Green, C. Yarish, J. Kim, & C.D. Neefus. 2014. New England seaweed
644 culture handbook: nursery systems. *Connecticut Sea Grant College Program.* CTSG-14-01. 92
645 pp. Available at: https://seagrant.uconn.edu/2014/01/01/new-england-seaweed-culture-
646 handbook-nursery-systems/
647 [dataset] Reed, Laura and Candace Oviatt. 2020. Graduate School of Oceanography Dock Data,
648 1977 to Present.
649 Ren, J. S., Stenton-Dozey, J., Plew, D. R., Fang, J., & Gall, M. (2012). An ecosystem model for
650 optimising production in integrated multitrophic aquaculture systems. *Ecological Modelling*,
651 246, 34-46.
652 Schaffelke, B., & Lüning, K. (1994). A circannual rhythm controls seasonal growth in the kelps
653 *Laminaria hyperborea* and *L. digitata* from Helgoland (North Sea). *European Journal of*
654 *Phycology*, *29*(1), 49-56.
655 Schiener, P., Black, K. D., Stanley, M. S., & Green, D. H. (2015). The seasonal variation in the
656 chemical composition of the kelp species *Laminaria digitata*, *Laminaria hyperborea*, *Saccharina*
657 *latissima* and *Alaria esculenta*. *Journal of Applied Phycology*, *27*(1), 363-373.

Segarra, K. E. A. 2002. Source Or Sink? Analysis of Narragansett Bay's carbon cycle. Brown University. Center for Environmental Studies.

Sjøtun, K. (1993). Seasonal lamina growth in two age groups of *Laminaria saccharina* (L.) Lamour. in western Norway. *Botanica marina*, *36*(5), 433-442.

Soetaert, K., & Petzoldt, T. (2010). Inverse modelling, sensitivity and Monte Carlo analysis in R using package FME. *Journal of Statistical Software*, *33*(3), 1-28.

Soetaert, K., Petzoldt, T. R., & Setzer, W. (2010). Solving Differential Equations in R: Package deSolve. Journal of Statistical Software, 33(9), 1-25. URL http://www.jstatsoft.org/v33/i09/ DOI 10.18637/jss.v033.i09

Taylor, W. R. (1972). *Marine algae of the eastern tropical and subtropical coasts of the Americas*. University of Michigan.

Townsend, D. W. (1991). Influences of oceanographic processes on the biological productivity of the Gulf of Maine. *Reviews in Aquatic Sciences*, *5*(3), 211-230.

Ullman, D. S. & Codiga, D. L. (2010) *Characterizing the Physical Oceanography of Coastal Waters Off Rhode Island, Part 2: New Observations of Water Properties, Currents, and Waves.* Retrieved from https://www.seagrant.gso.uri.edu/oceansamp/pdf/appendix/03-PhysOcPart2-OSAMP-UllmanCodiga2010.pdf

Vettori, D., & Nikora, V. (2017). Morphological and mechanical properties of blades of *Saccharina latissima*. *Estuarine, Coastal and Shelf Science*, *196*, 1-9.

Wu, R. S. S. (1995). The environmental impact of marine fish culture: towards a sustainable future. *Marine Pollution Bulletin*, *31*(4-12), 159-166.

Tables

Table 1. Model equations with environmental conditions: T = temperature (K), I = irradiance (mol γ m^{-2} h^{-1}), DIC = dissolved inorganic carbon (mol DIC L^{-1}), and N = nitrate and nitrite concentration (NO_3^- and NO_2^- L^{-1}).

Equation	Description
$C_T = exp\left(\frac{T_A}{T_0} - \frac{T_A}{T}\right)\left[1 + exp\left(\frac{T_{AL}}{T_0} - \frac{T_{AL}}{T_L}\right) + exp\left(\frac{T_{AH}}{T_H} - \frac{T_{AH}}{T_0}\right)\right]\left[1 + exp\left(\frac{T_{AL}}{T} - \frac{T_{AL}}{T_L}\right) + exp\left(\frac{T_{AH}}{T_H} - \frac{T_{AH}}{T}\right)\right]^{-1}$	Temperature correction
$j_{E_NA} = j_{E_NAm} C_T \frac{[N]}{[N] + K_N}$	Specific assimilation rate of N
$j_{CO_2} = j_{CO_2m} C_T \frac{[DIC]}{[DIC] + K_C}$	Specific CO_2 uptake rate from photosynthetic SU1
$j_I = \frac{\rho_{PSU} I\dot{b}_I \alpha_I}{1 + \frac{I\dot{b}_I \alpha_I}{\dot{k}_I C_T}}$	Specific relaxation rate from photosynthetic SU2
$j_{O_2} = \frac{M_V}{W} j_I y_{LO_2} w_{O_2}$	Oxygen production rate
$j_{E_CA} = \left(\frac{1}{j_{E_CAm} C_T} + \frac{1}{j_{CO_2}/y_{CO_2C}} + \frac{1}{j_I/y_{IC}} - \frac{1}{j_I/y_{IC} + j_{CO_2}/y_{CO_2C}}\right)^{-1}$	Specific assimilation rate of C from photosynthetic SU3
$j_{E_iC} = m_{E_i}\left(\dot{k}_{Ei} C_T - \dot{r}\right)$	Specific catabolic flux of N or C reserve
$\dot{r} = \frac{1}{M_V}\frac{dM_V}{dt}$	Net specific growth rate
$j_{E_i}^{M_i} = \min\left(j_{E_iC}, j_{E_iM} C_T\right)$	Specific maintenance flux from N or C reserve
$j_{E_iG} = j_{E_iC} - j_{E_i}^{M_i}$	Specific growth flux from N or C reserve
If $j_{E_i}^{M_i} < j_{E_iM} C_T$ $j_V^M = \sum_i j_{V_i}^{M_i} = \sum_i \left[\left(j_{E_iM} C_T - j_{E_i}^{M_i}\right) y_{E_iV}^{-1}\right]$	Specific maintenance flux from structure

$j_{VG} = \left[\sum_i \left(\frac{j_{E_iG}}{y_{E_iV}}\right)^{-1} - \left(\sum_i \frac{j_{E_iG}}{y_{E_iV}}\right)^{-1}\right]^{-1} = \dot{r} + j_V^M$	Gross specific growth rate
$j_{E_iR} = j_{E_iG} - y_{E_iV}\, j_{VG}$	Specific flux of rejected C or N from growth SU
$\frac{d}{dt} m_{E_i} = j_{E_iA} - j_{E_iC} + \kappa_{E_i} j_{E_iR} - \dot{r}\, m_{E_i}$	Dynamics of the N or C reserve
$\frac{d}{dt} M_V = \dot{r} M_V$	Dynamics of structural mass
$W_d = (w_V + m_{E_C} w_{EC} + m_{E_N} w_{EN}) M_V$	Whole *S. latissima* blade dry weight
$L_w = \left(\frac{W_d}{3.87\ 10^{-3}}\right)^{\frac{1}{1.469}}$	Physical length

Table 2. *S. latissima* DEB model parameters and units resulting from fitting the model to the compiled literature and field data.

Parameter	Parameter description	Parameter Units	Value	Source
j_{E_NAm}	Maximum volume specific nitrogen assimilation	mol N mol V^{-1} h^{-1}	1.5 * 10^{-4}	Fitted from data by Espinoza and Chapman (1983)
K_N	Half-saturation concentration for NO_3^- and NO_2^- uptake	mol NO_3^- and NO_2^- L^{-1}	2.5 * 10^{-6}	Fitted from data by Espinoza and Chapman (1983)
j_{CO_2m}	Maximum volume specific CO_2 uptake rate	mol CO_2 mol V^{-1} h^{-1}	0.0075	This study
K_C	Half-saturation concentration for CO_2 uptake	mol CO_2 L^{-1}	4 * 10^{-7}	This study
ρ_{PSU}	Photosynthetic unit (PSU) density	mol PSU mol V^{-1}	0.5	Fitted from data by Johansson and Snoeijs (2002)
$\dot{b}_I$	Binding probability of a photon	-	0.5	Fitted from data by

	to a free light SU			Johansson and Snoeijs (2002)
$\boldsymbol{\alpha_I}$	Specific photon arrival cross section	m^2 mol PSU^{-1}	1	Fitted from data by Johansson and Snoeijs (2002)
$\boldsymbol{\dot{k}_I}$	Dissociation rate of photosynthetic products	mol γ mol PSU^{-1} h^{-1}	0.075	Fitted from data by Johansson and Snoeijs (2002)
$\boldsymbol{y_{IC}}$	Yield of C reserve per photon	mol γ mol C^{-1}	10	Lavaud et al. (2020)
$\boldsymbol{y_{CO_2C}}$	Yield of C reserve per CO_2	mol CO_2 mol C^{-1}	1	Lavaud et al. (2020)
$\boldsymbol{y_{LO_2}}$	Yield factor of photon to O_2	mol O_2 mol γ^{-1}	0.125	Lavaud et al. (2020)
$\boldsymbol{j_{E_CAm}}$	Maximum volume specific carbon assimilation	mol C mol V^{-1} h^{-1}	0.282	This study
$\boldsymbol{\dot{k}_{EN}}$	N reserve turnover rate	h^{-1}	0.04	Lavaud et al. (2020)
$\boldsymbol{\dot{k}_{EC}}$	C reserve turnover rate	h^{-1}	0.02	Lavaud et al. (2020)
$\boldsymbol{j_{E_NM}}$	Volume specific maintenance cost paid by N reserve	mol N mol V^{-1} h^{-1}	$4 * 10^{-6}$	This study
$\boldsymbol{j_{E_CM}}$	Volume specific maintenance cost paid by C reserve	mol C mol V^{-1} h^{-1}	$1 * 10^{-6}$	This study
$\boldsymbol{y_{E_NV}}$	Yield factor of N reserve to structure	mol N mol V^{-1}	0.04	Lorena et al. (2010)
$\boldsymbol{y_{E_CV}}$	Yield factor of C reserve to structure	mol C mol V^{-1}	1	This study
$\boldsymbol{\kappa_{E_i}}$	Fraction of rejection flux incorporated back in i-reserve	-	0.9	This study
$\boldsymbol{T_A}$	Arrhenius temperature	K	6314.3	This study
$\boldsymbol{T_0}$	Reference temperature	K	293.15	This study

T_H	Upper boundary of temperature tolerance	K	286.536	This study
T_L	Lower boundary of temperature tolerance	K	273.15	This study
T_{AH}	Arrhenius temperature outside T_H	K	18702	This study
T_{AL}	Arrhenius temperature outside T_L	K	4391.9	This study
w_V	Molar weight of structure	g mol V^{-1}	29.89	C:H:O:N; 1: 1.33:1:0.04
w_{EC}	Molar weight of C reserve	g C mol C^{-1}	54	C:H:O:N; 1:2:1:0
w_{EN}	Molar weight of N reserve	g N mol N^{-1}	17	C:H:O:N; 0:0:2.5:1
w_{O_2}	Molar weight of O_2	g O_2 mol O_2^{-1}	32	Periodic table

686

687 **Table 3.** Data from literature and this study used to calibrate the *S. latissima* DEB model.

Reference	Location	Data	Experimental conditions	Time period
Espinoza and Chapman (1983)	Nova Scotia, Canada	NO^{3-} uptake (µg N g_{DW}^{-1} h^{-1})	T = 9 and 18 °C [N] = from 2.5 to 88 * 10^{-6} M NO^{3-}	Discrete measurements
Johansson and Snoeijs (2002)	Sweden	Measured O_2 evolution (µmol O_2 kg DW^{-1} s^{-1})	T = 14 °C I = 0-900 µE m^{-2} s^{-1}	Discrete measurements
*Davison (1987)	Germany	Photosynthesis rates (µmol C g_{ww}^{-1} h^{-1})	T = 0-30 °C with 5 °C intervals I = 200 µE m^{-2} s^{-1}	Discrete measurements
*Fortes and Lüning (1980)	Germany	Specific growth rate (% d^{-1})	T = 0, 5, 10, 15, and 20 °C I = 70 µE m^{-2} s^{-1}	7 days

*Bolton and Lüning (1982)	Germany, UK, France, and Norway	Specific growth rate (% d^{-1})	T° = 0, 5, 10, 15, 20, and 23 °C I = 50 µE m^{-2} s^{-1}	7 days
*Davison and Davison (1987)	Germany	Relative growth rate (cm cm^{-1} $month^{-1}$)	T = 0, 5, 10, 15 and 20 °C I = 60 µE m^{-2} s^{-1}	1 month
This study	Rhode Island, USA	Blade length (cm) and N:C ratio (mol mol^{-1})	T = 1.5-20 °C [N] = 0-1 * 10^{-5} mol NO_3^- and NO_2^- L^{-1} [C] = 1.836 * 10^{-3} mol DIC L^{-1} at Pt. Judith Pond sites and 1.956 * 10^{-3} mol DIC L^{-1} for Narragansett Bay sites I = 0-2 * 10^6 daily µE m^{-2} h^{-1}	138- 172 days

*Used only to build the Arrhenius relationship.

Table 4. Length of *S. latissima* blades in cm (± SD) at the end of the growing season in each site.

Site	Year 1	Year 2
Narragansett Bay North	67.9 (± 22.6)	50.5 (± 13.0)
Narragansett Bay South, Line 1	133.4 (± 78.8)	65.3 (± 22.5)
Narragansett Bay South, Line 2	73.2 (± 17.6)	20.0 (± 6.8)
Pt. Judith Pond North, Line 1	74.8 (± 18.3)	80.1 (± 23.1)
Pt. Judith Pond North, Line 2	81.0 (± 34.8)	46.9 (± 14.7)
Pt. Judith Pond South, Line 1	85.9 (± 37.1)	63.8 (± 26.3)
Pt. Judith Pond South, Line 2	87.3 (± 32.0)	47.1 (± 10.9)

691 **Figures**

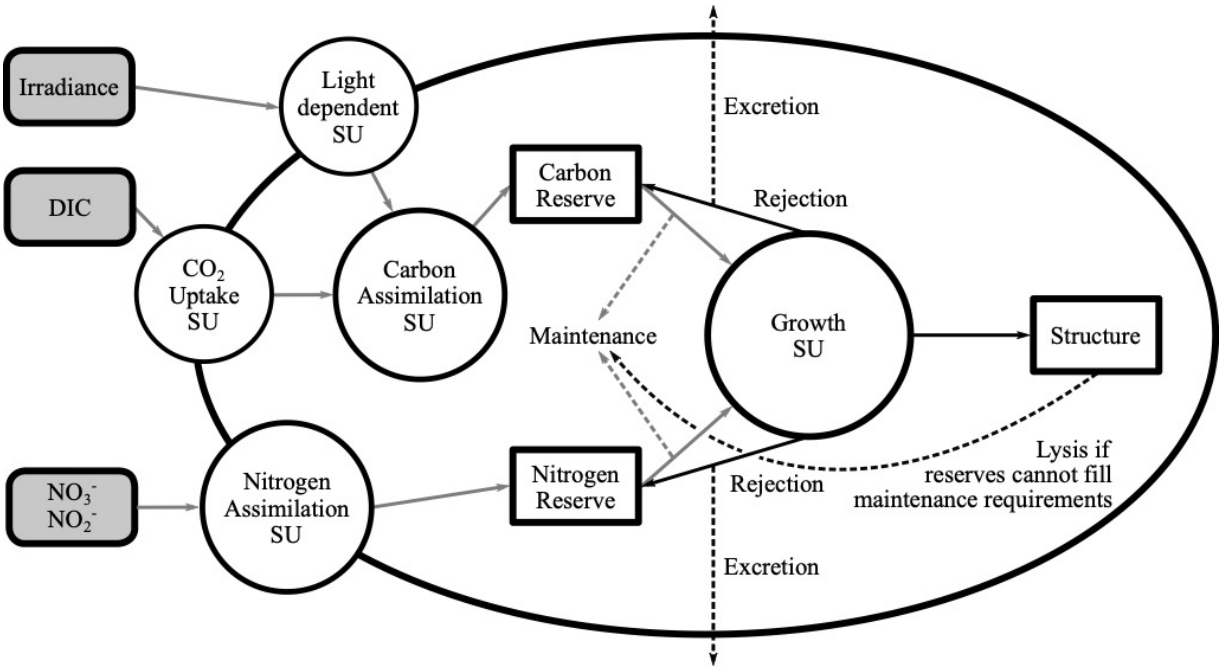

692
693 **Figure 1.** *S. latissima* DEB model conceptual framework (adapted from Lavaud et al., 2020).
694 The large oval represents the algae and the surrounding area is its environment. Grey rounded
695 rectangles are the model forcing variables. White rectangles are the state variables of the model,
696 representing the main pools of mass in the modeled organism. Circles are synthesizing units,
697 processing key metabolic transformations. Dotted arrows represent fluxes of mass leaving the
698 main model system either through excretion or use in maintenance. Grey arrows depict where the
699 temperature correction is applied to a reaction.

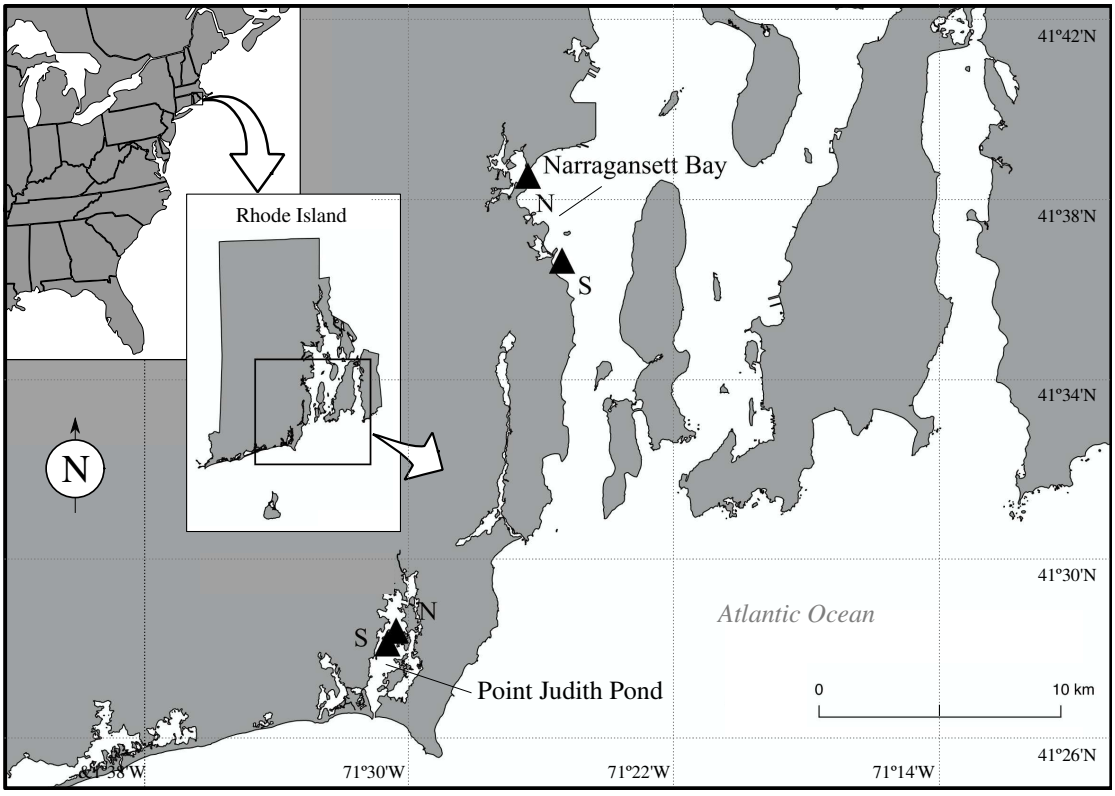

700

701 **Figure 2.** Map of growing sites (triangles) for *S. latissima* on Rhode Island oyster farms.

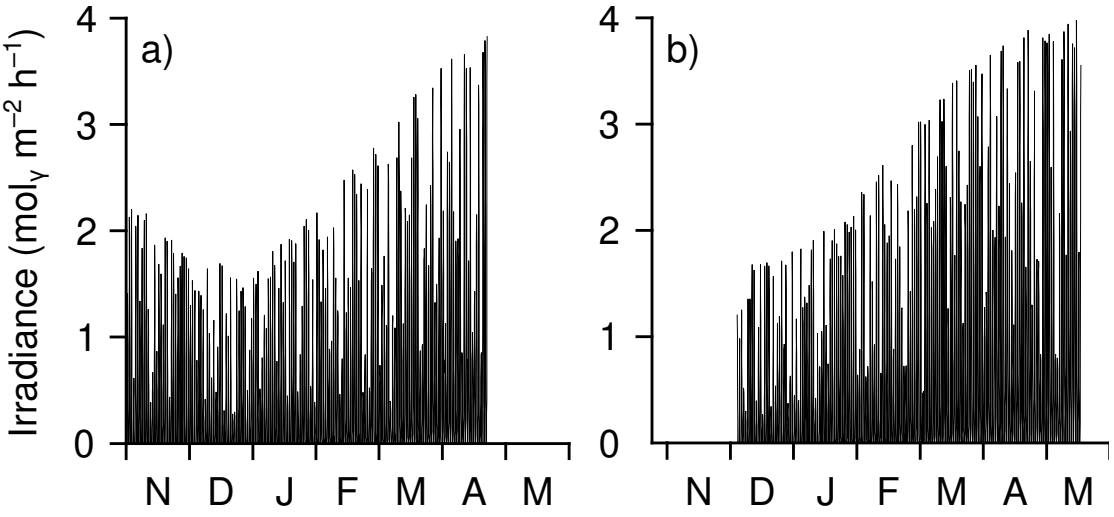

702

703 **Figure 3.** Irradiance forcing used in all sites for year 1 (a) and year 2 (b) of the field study

704 converted from the radiative forcing from the North American Regional Reanalysis.

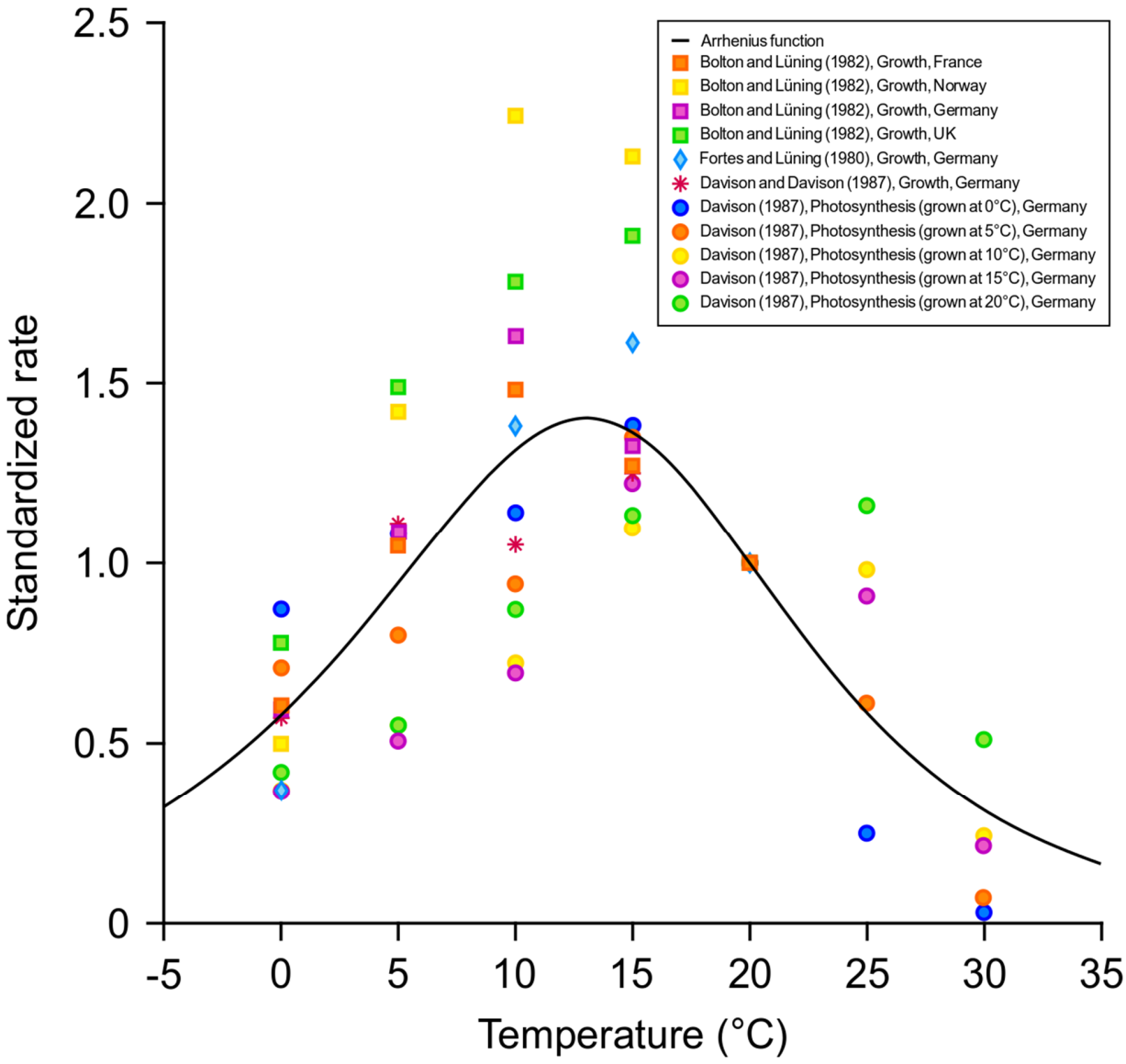

Figure 4. Arrhenius relationship for *S. latissima* estimated using multiple growth and photosynthesis datasets from: Bolton and Lüning (1982; squares; orange for kelp from France, yellow for Norway, purple for Germany, green for the UK), Fortes and Lüning (1980; blue diamonds), Davison and Davison (1987; red asterisk), and Davison (1987 circles; blue for sporophytes rearing temp 0 °C, orange for 5 °C, yellow for 10 °C, purple for 15 °C, and green for 20 °C). The adjusted R-squared statistic for the fit of the curve to the data points is 0.551 (p-value = $2.74\ 10^{-11}$).

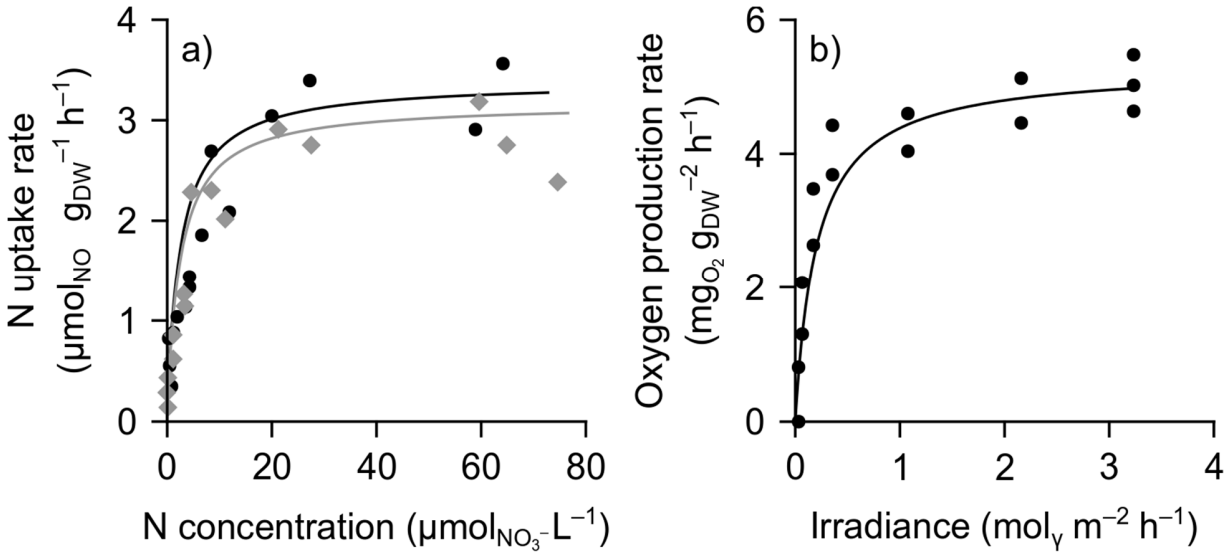

713

714 **Figure 5.** Predicted (lines) and observed (points) a) N uptake from Espinoza and Chapman

715 (1983) at 9 °C (black circles) and 18 °C (grey diamonds) and b) Oxygen production from

716 Johansson and Snoeijs (2002).

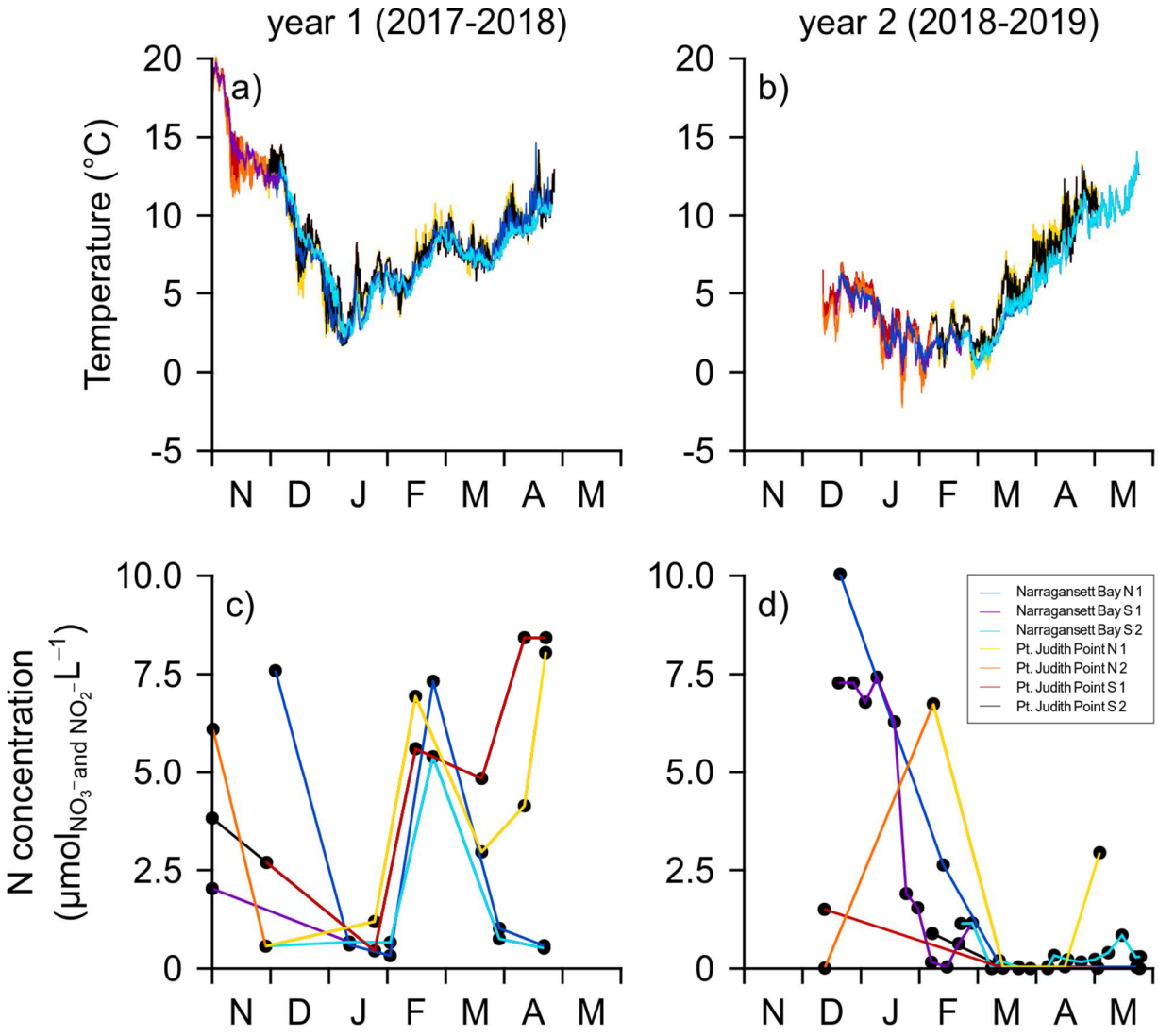

Figure 6. Measured temperature (°C; a,b) and nitrate and nitrite concentrations (μmol L^{-1}; c,d) from year 1 (left panels) and year 2 (right panels). Narragansett Bay lines are in dark blue (North site 1), purple (South site 1), and light blue (South site 2). Pt. Judith Pond lines are in orange (North site 1), yellow (North site 2), brown (South site 1) and black (South site 2). Observed N concentrations are indicated by black dots.

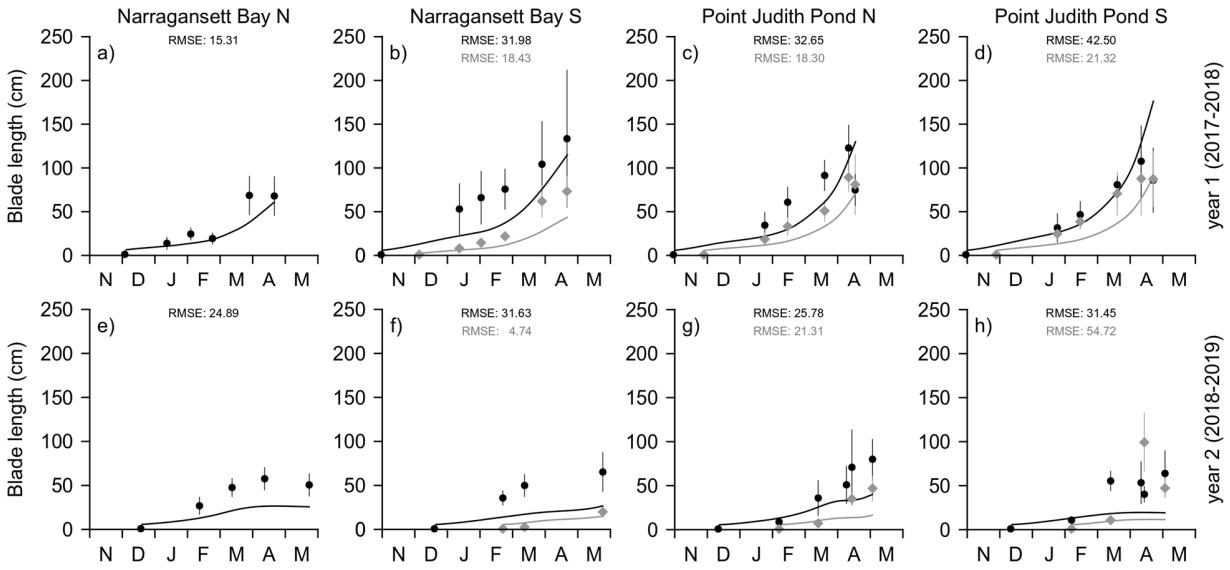

Figure 7. *Saccharina latissima* blade length (cm) during year 1 (top row) and year 2 (bottom row). Dots and diamonds with error bars depict the mean observed length from the field data and their standard deviation, respectively. Lines are the predicted length from the *S. latissima* DEB model. Lines and dots in black are the first *S. latissima* line planted at a site, and lines and diamonds in grey depict the second *S. latissima* line planted later in the year.

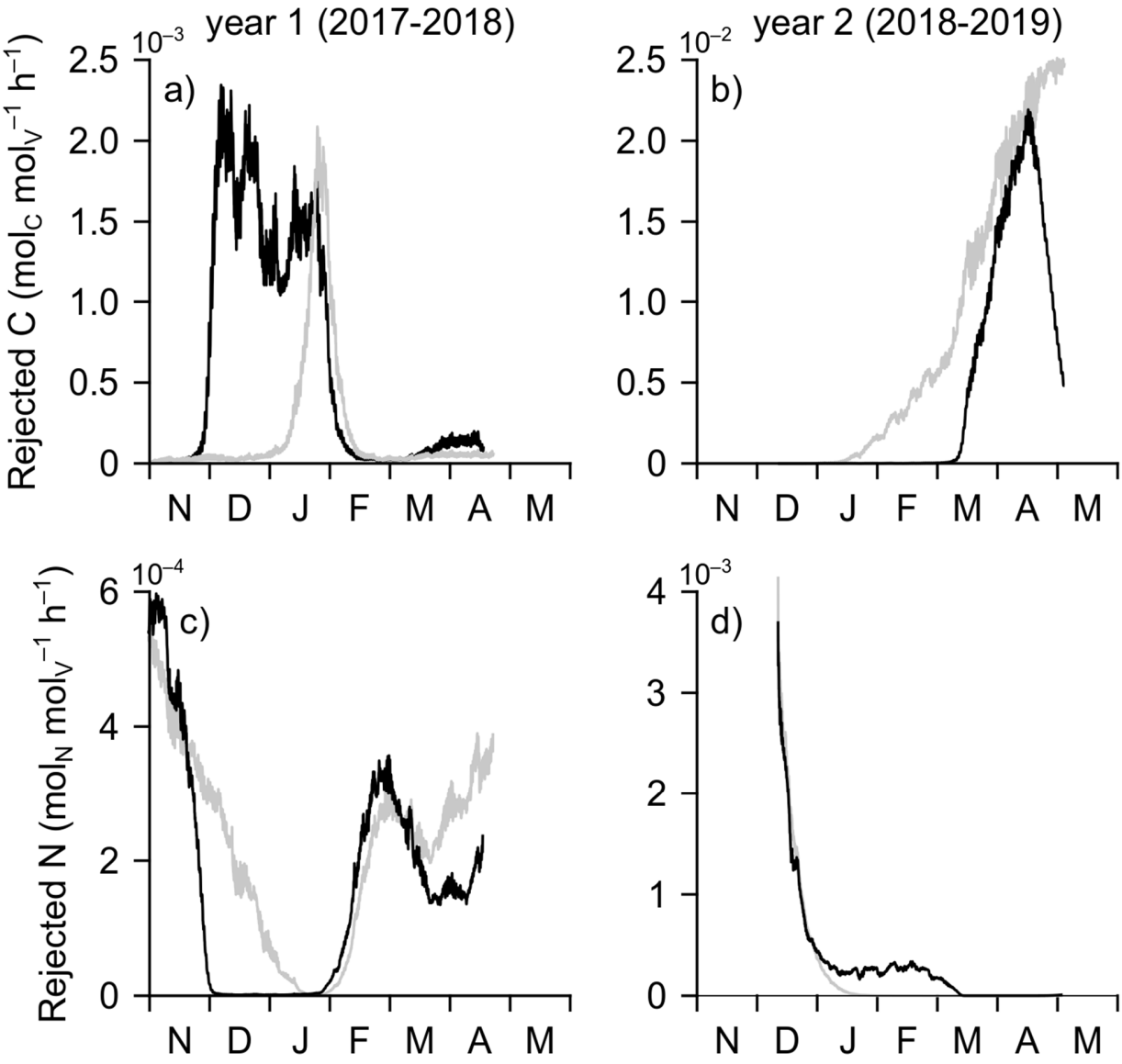

729

730 **Figure 8**. Rejected fluxes of C (a,b) and N (c,d) from the growth SU back to reserves at Pt.

731 Judith Pond in year 1 (left panels) and year 2 (right panels). Black is for the North *S. latissima*

732 line and the grey is for the South line on all plots.

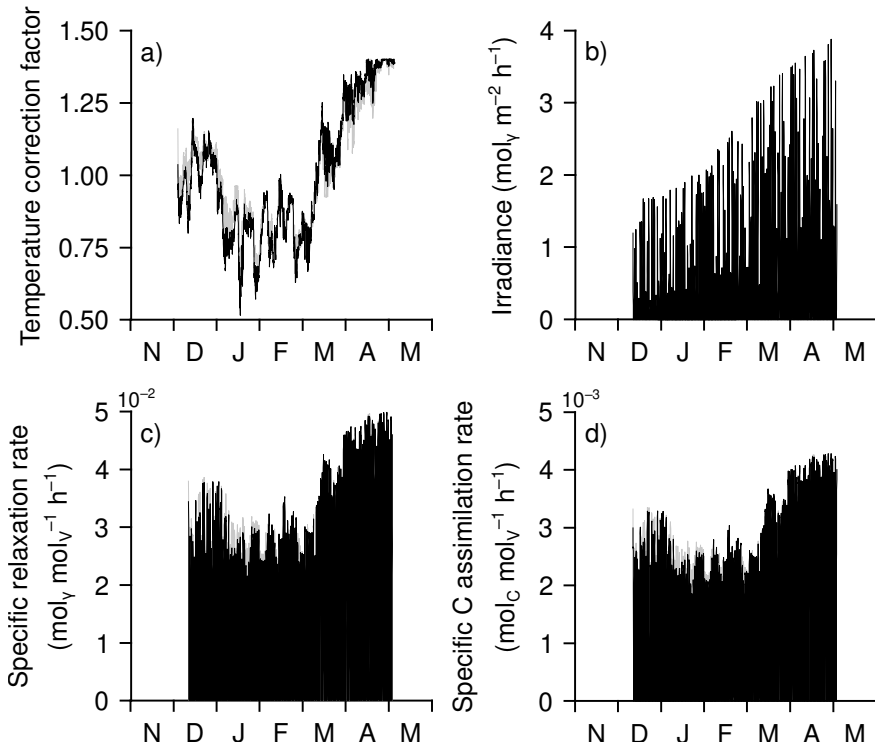

733

734 **Figure 9.** Temperature correction factor (a), irradiance (b), specific relaxation rate from

735 photosynthetic SU2 (c) and carbon assimilation rate resulting from photosynthetic SU3 (d) at Pt.

736 Judith Pond during year 2. Black is for the North *S. latissima* line and the grey is for the South

737 line.

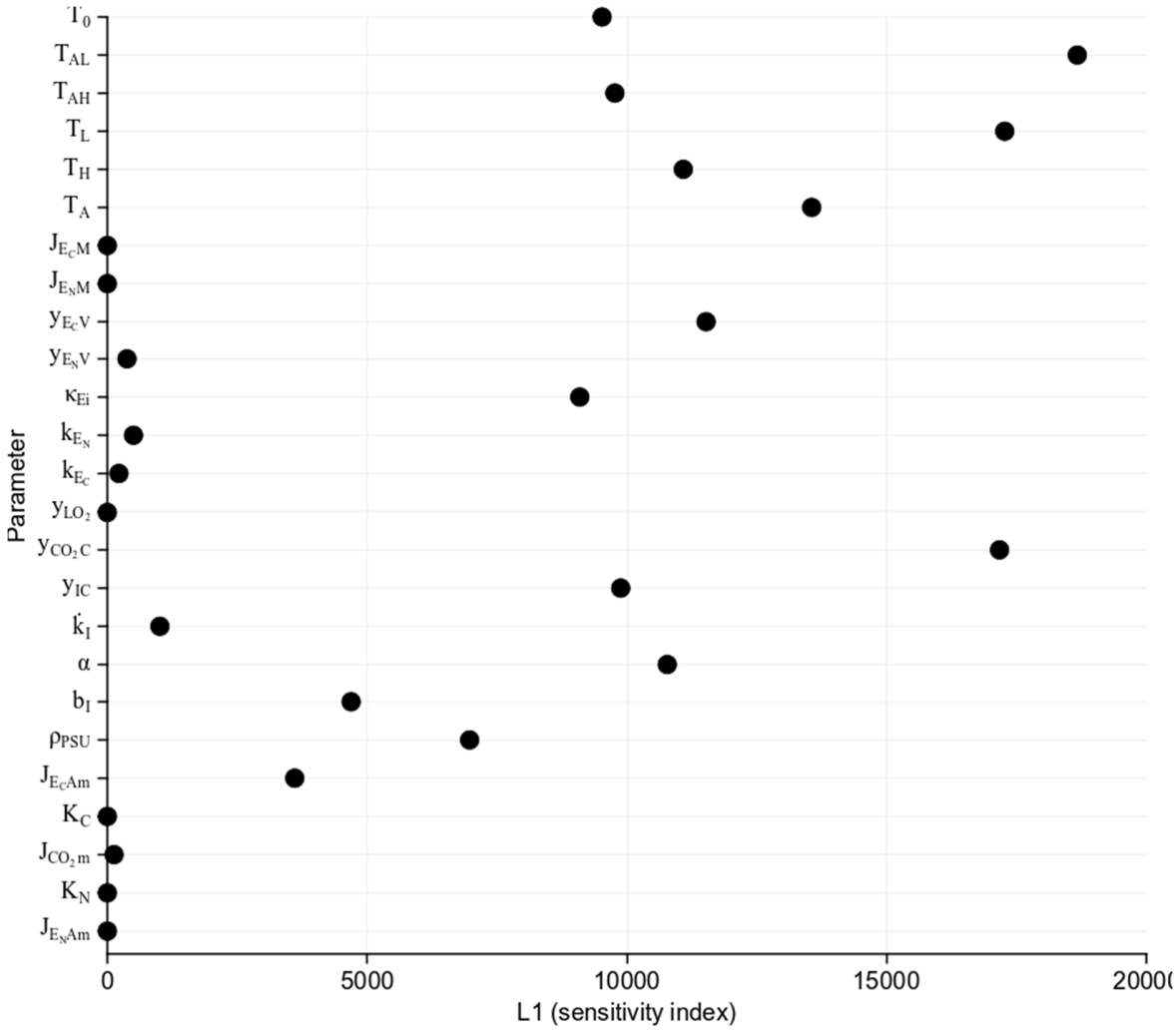

738

739 **Figure 10**. Graphic presentation of the results of the sensitivity analysis of the state variables

740 $\boldsymbol{m_{E_C}}$, $\boldsymbol{m_{E_N}}$, and $\boldsymbol{M_V}$ to model parameters as measured by the L1 sensitivity function.